Torque Ripple Minimization in SRMs at Medium and High Speeds using a Multi-Stator Windings with a Novel Power Converter

Oguzhan Kilic[(1)] Ali Elrayyah[(2)] Yilmaz Sozer[(1)]

[(1)] Electrical and Computer Engineering Department
The University of Akron, Akron, USA

[(2)] Qatar Environment and Energy Research Institute
Doha, Qatar

***Abstract*— In this paper, a switched reluctance motor (SRM) with a new winding configuration and a novel power converter topology is presented. The new winding topology along with the power converter are developed to improve the machine efficiency by exciting only the portion of the phase windings at high speeds. The new configuration helps overcoming the effect of the high back EMF (Electromotive Force) and hence improving the torque speed characteristics of the SRM. The proposed configuration is investigated using coupled Finite Element Analysis (FEA) and circuit simulations on a case study motor. The new SRM drive and its associated control have been experimentally tested.**

***Keywords*— High speed SRM, Switched reluctance machine, Torque ripple minimization.**

I. Introduction

Switched reluctance machines (SRMs) have been extensively used in many applications like aerospace, hybrid electric vehicles and wind power generation [1-3]. SRMs have outstanding inherent characteristics such as simple mechanical structure, reliability, wide speed operation and robustness [4]. The mechanical torque in SRMs is developed by the tendency of the rotor to move in order to maximize the inductance of the excited winding [5]. Individual phase excitations should be controlled in a sequential pattern in order to maintain the flow of the positive torque production and to avoid the introduction of the negative torque.

Despite the fact that SRMs are good candidates for high speed applications as they have higher efficiency, higher starting torque and competent high speed characteristics; they suffer from the poor torque production at high speeds, as a result of the short excitation time, slow demagnetization and high back EMF voltages [6]. Beside these disadvantages of SRMs at high speed operation; they also encounter high torque ripple and high acoustic noise problems [7].

The proposed winding configuration; along with the new converter design are developed to address the problems associated with the high speed operation in SRMs. The typical driver used for SRMs is an asymmetric converter which is composed of two switches and two diodes in each phase as shown in Fig.1 [8]. The two switches are used to control the excitation current developed in each phase while the diodes provide the discharge path for the current in the freewheeling and the demagnetization modes [8].

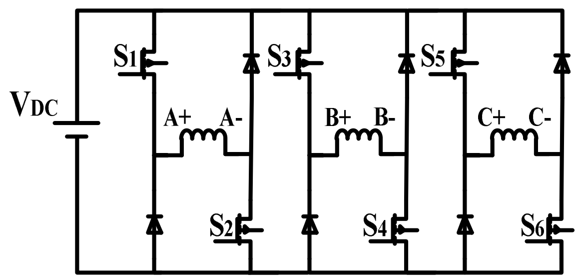

Fig. 1. Typical SRM power converter.

One of the factors that effects the performance of an SRM is the number of turns *Ns* used in the stator coils. Higher *Ns* values in the stator of the machine help producing higher torques at low speeds. On the other hand, higher *Ns* prevents producing the phase currents and the torque at high speed operations. In this paper, the objective is to use multi-windings per phase in the stator such that at low speed operation, higher number of turns is used while at high speed low number of turns is considered. In order to implement this control strategy a new converter design with an extra switch in each phase and its associated control algorithm are presented.

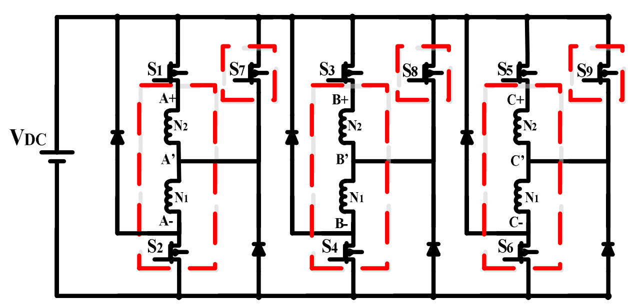

Fig. 2. Proposed converter design.

II. Proposed Winding Configuration And Novel Converter Design

The proposed converter design along with the winding topology is presented in Fig. 2. The phase windings are separated according to the system requirements by connecting the two diodes across portion of the windings that will be used for the demagnetization and will be excited during the high speed operation. To achieve different number of turns for different speed ranges an extra switch (S7) is needed. The rated current of S7 is much lower than that of the other switches (S1 and S2) as it carries current only during high speeds which is much lower than the rated current of the inverter. Clearly, for low speed high torque operation, the switches S1 and S2 are used as shown in Fig. 3, while at high speeds the switches S7 and S2 should be used as shown in Fig 4.

For the freewheeling mode in phase A; S2 is switched ON and OFF to regulate the current according to the predefined current reference as shown in Fig. 5 for low speeds, while S7 is used for the same purpose at high speeds as shown in Fig. 6.

For the demagnetization mode in phase A; the portion of the windings defined by *N1* is used to discharge the current in both high and low speeds as shown in Fig. 7. The demagnetization capabilities at low speeds is improved as the phase current is discharged through less number of turns and hence high voltage/turn ratio will be applied during the demagnetization.

The main purpose of the proposed topology is to give more room for the current to build to higher values at high speeds, which can provide higher torque density and better torque profile. The advantage of this method is to reduce the flux linkage by decreasing the number of turns according to Eqn.1 [9]:

$$\lambda_a = N\emptyset \tag{1}$$

$$\frac{d\lambda}{dt} = \frac{d\lambda}{di}\frac{di}{dt} + \frac{d\lambda}{d\theta}\frac{d\theta}{dt} = l\frac{di}{dt} + \omega\frac{d\lambda}{d\theta} \tag{2}$$

$$T_e = \frac{1}{2}\frac{\frac{d\lambda_a(\theta)}{d\theta}}{d\theta}\, i_a \tag{3}$$

Where *l* is the incremental inductance and *θ*, *ω* and *Te* are the rotor position, motor speed and the average torque produced by phase A respectively. From Eqns.1 and 2; by reducing the number of turns the total flux linkage for a phase will decrease which will drop the back EMF voltage as defined by the second term in right hand side in Eqn. 2. Increase in the instantaneous current should increase the torque production, but from Eqn. 3; the torque could decrease due to the reduction in the number of turns. Further analysis would require to optimize the selection for the turns ratio between the two windings in each phase in order to compromise between the gain in the torque by boosting the current and the reduction in the torque by sacrificing some of the windings turns. For the torque ripple improvement can be defined as [7]:

$$\text{Torque Ripple} = \frac{T_{inst}(max)\text{-}\,T_{inst}(min)}{T_{avg}} \times 100\% \tag{4}$$

The average torque will increase along with the instantaneous maximum and minimum torque which should minimize the torque ripple.

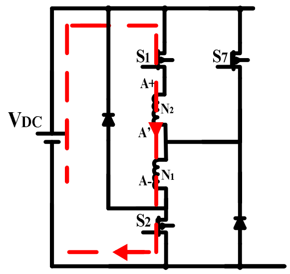

Fig. 3. Low speed magnetization.

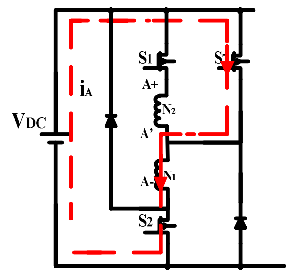

Fig. 4. High speed magnetization.

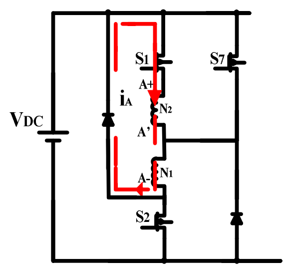

Fig. 5. Low speed free-wheeling.

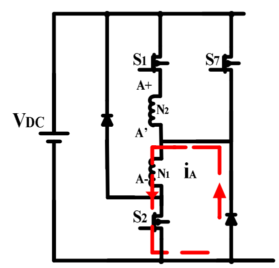

Fig. 6. High speed free-wheeling.

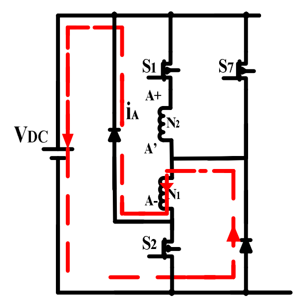

Fig. 7. Low and high speed demagnetization.

III. Torque Speed Analysis With Multi-Stator Configuration

The proposed multi-stator windings with the new power converter are designed to improve the machine performance at high speeds by boosting the excitation current to levels that cannot be reached in the normal single pulse operation at high speeds. In the low speed regions the machine operation is similar to the conventional SRM, except during the demagnetization. The proposed system boosts the negative voltage applied to the secondary windings to discharge the current and provides a shorter time to discharge the phase currents compared to the typical time elapsed with the conventional machine as shown in Fig. 8. Phase currents in both the new system and the conventional machine for medium and high speeds are depicted in Fig. 9 and 10 respectively. Where *Ia*, and *Ia1* denote the currents in the conventional machine windings, and primary windings in the multi-stator machine respectively.

At the high speed regions the power converter control excites just the primary windings which has the higher number of turns. The improvement in the current profile is shown in Fig. 9 and 10 as the current builds to higher values. The higher current values enhance the average torque production and enables the driver to control the current and hence minimize the torque ripple and the acoustic noise usually associated with the SRM operation.

The same turn-on, turn-off angles along with the same current reference are applied for the both cases for the sake of comparison. For the SRM used in this study the high speed was defined to be 2000 rpm and higher. The comparison between the flux linkages are shown in the Fig. 11-13 for different speeds. It is an important advantage that the new system can improve the SRM torque characteristics at high speed using the same machine design; by changing the winding configuration and using one extra switch per phase.

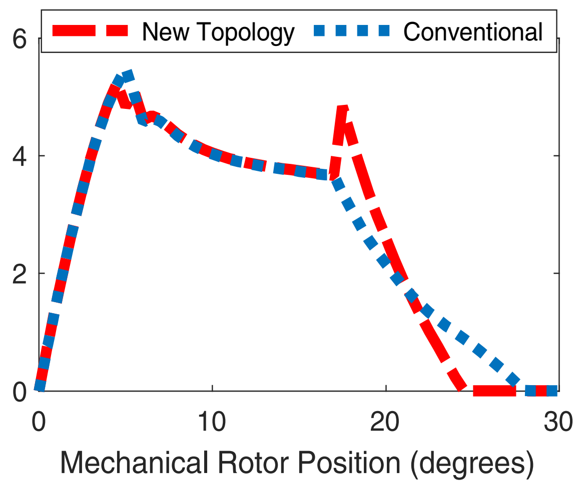

Fig. 8. Phase currents at 1000 rpm.

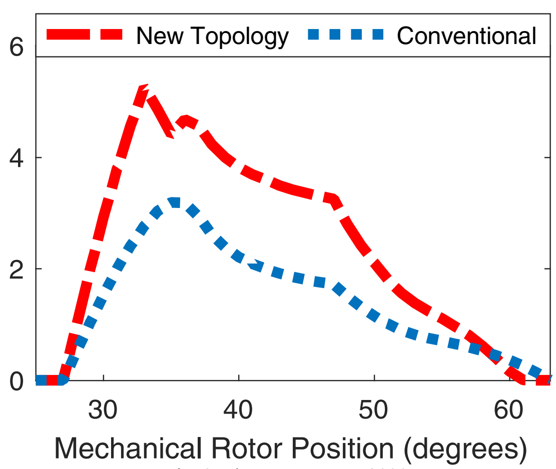

Fig. 9. Phase currents at 3000 rpm.

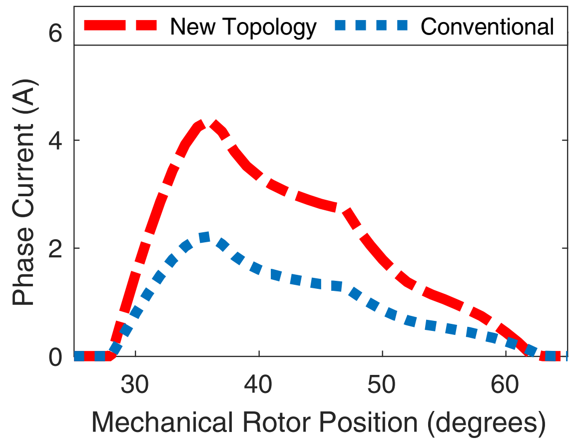

Fig. 10. Phase currents at 4000 rpm.

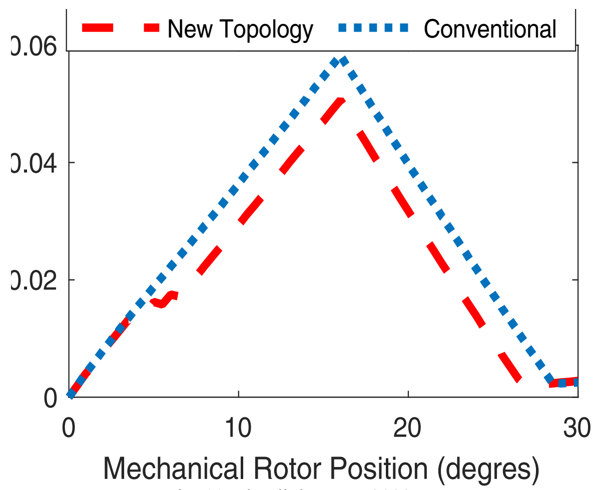

Fig. 11. Flux linkages at 2000 rpm.

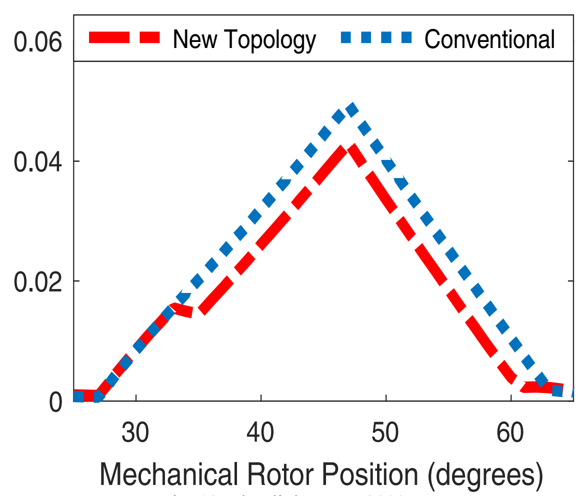

Fig. 12. Flux linkages at 3000 rpm.

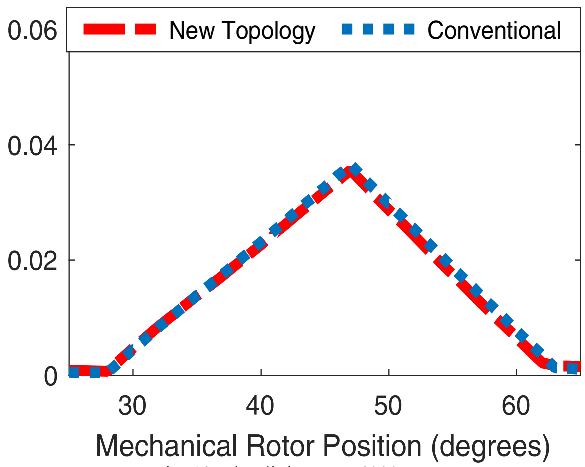

Fig. 13. Flux linkages at 4000 rpm.

IV. CASE STUDY

Case study for a 12-8, 100 W 1000 rpm motor was designed in Flux2D FEA (Finite Element software for electromagnetic and thermal analysis) as shown in Fig. 14 to investigate the competency of the winding configuration along with the new power converter design for the SRM. The total slot area for the machine model was 104 mm^2 which was divided as 69.3 mm^2 for the primary windings and 34.7 mm^2 for the secondary windings according to the number of turns distribution between them; for N1= 100 and N2=50 turns.

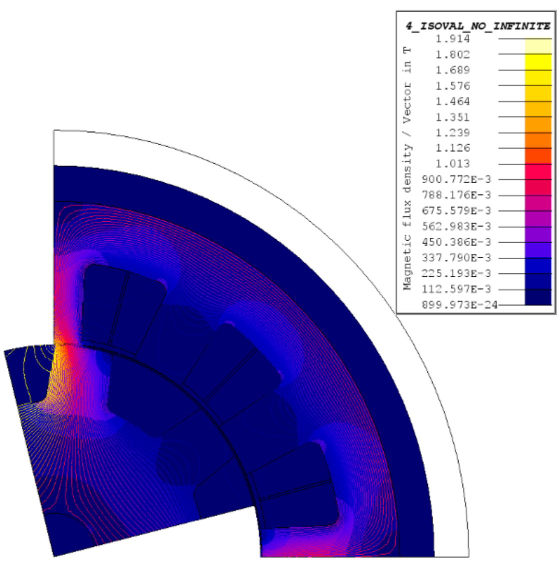

Fig. 14. SRM Finite Element model.

The FEA model was interfaced with a power converter in Flux using the electrical circuit simulator and its associated control. The converter reference current was chosen to be 5 A with a current density limit of 3.4 A/mm^2, while the converter DC voltage was set to be 50 V. The torque ripple comparisons for the case study under different speeds are presented in Fig. 15-17.

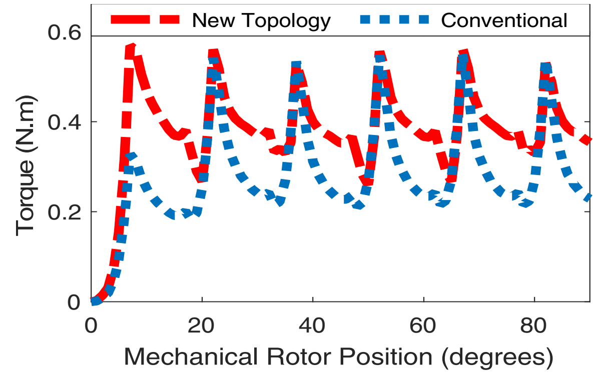

Fig. 15. Torque comparison at 2000 rpm.

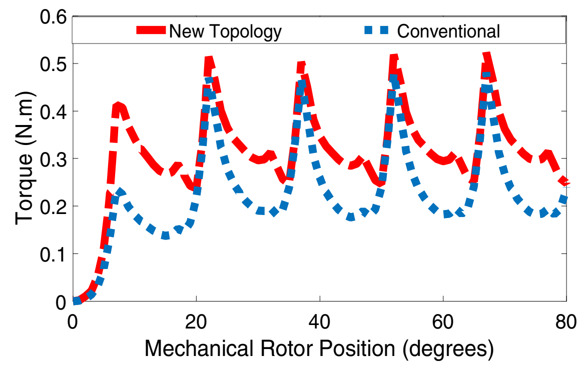

Fig. 16. Torque comparison at 3000 rpm.

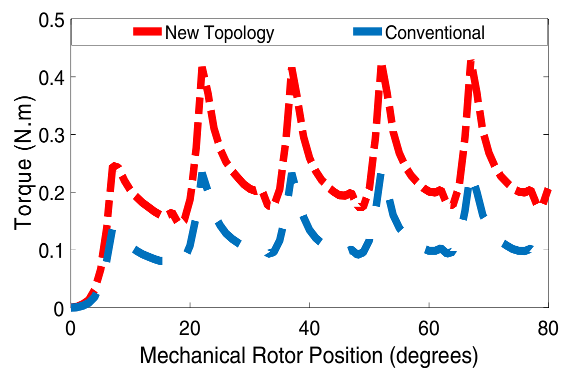

Fig. 17. Torque comparison at 4000 rpm.

V. EXPERIMENTAL RESULTS

The 12/8 100W SRM with multi winding is experimentally tested via extra switch novel converter. To apply the control algorithm, DSpace 1401 MicroAuto box is used. Fig. 18 shows the experimental setup that contains multi winding SRM, extra switch novel converter, DSpace controller, and the controllable mechanical load. The specification of the experimental SRM is provided in Table 1.

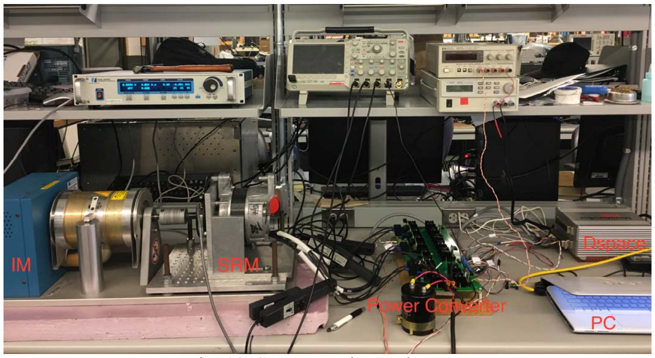

Fig. 18. SRM experimental setup.

Both the conventional and proposed SRM configuration drived with same optimum excitation angles. Fig. 19-21 present the current profiles for conventional and proposed systems respectively at different operating speeds.

Table 1. Specifications of the experimental SRM

Quantity	Value	Units
Rated Power	100	Watts
Based Speed	1000	rpm
Maximum Speed	4000	rpm
DC Voltage	50	Volts
Number of Stator Poles	12	
Number of Rotor Poles	8	
Number of Phases	3	

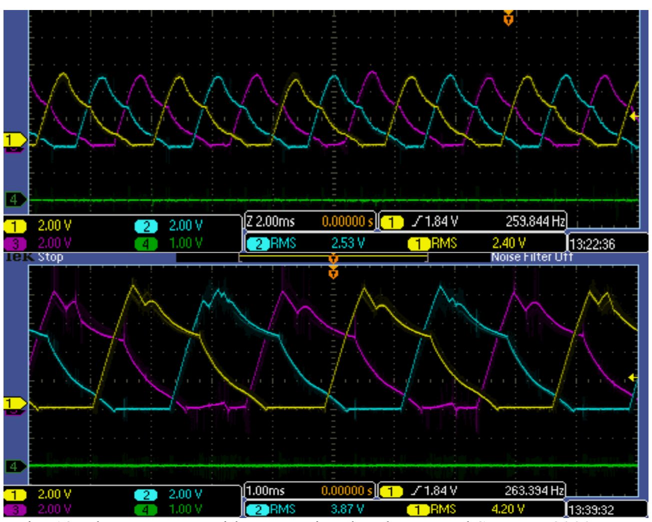

Fig. 19. Phase currents with conventional and proposed SRMs at 2000 rpm.

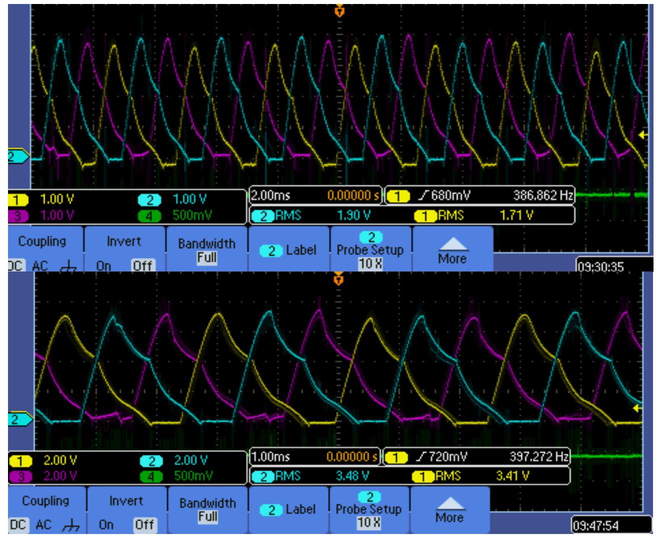

Fig. 20. Phase currents with conventional and proposed SRMs at 3000 rpm.

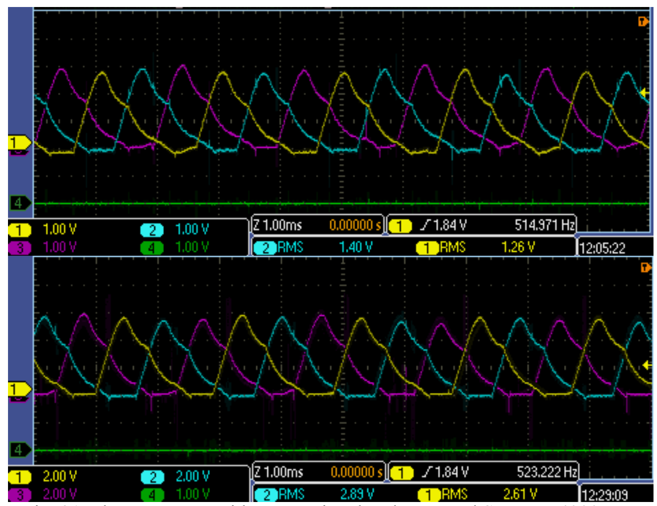

Fig. 21. Phase currents with conventional and proposed SRMs at 4000 rpm.

The torque and power density improvements at high speeds are plotted in terms of comparison between the power and torque-speed curves for the both cases in Fig. 22 and 23 respectively. The FEA model was verified experimentally on a 100 W 12/8 SRM machine. The percentage of the error between the FEA model and the experimental setup was found to be within 10% for different loading conditions as shown in Fig. 24.

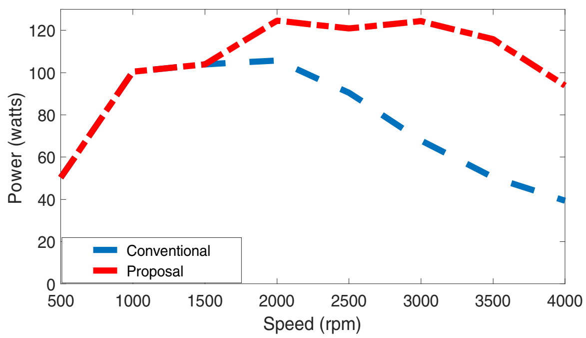

Fig. 22. Power speed curves of the proposed and the conventional SRMs

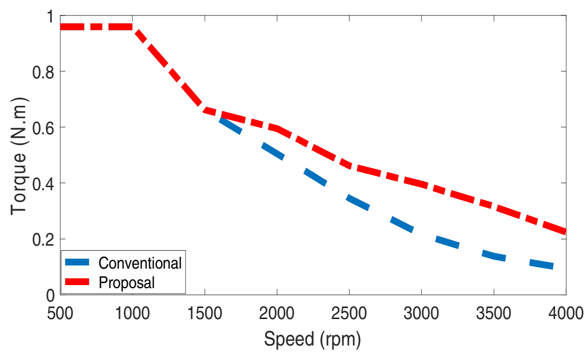

Fig. 23. Torque speed curves of the proposed and the conventional SRMs.

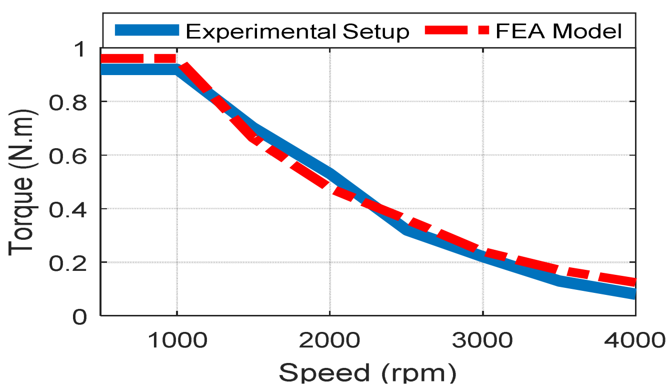

Fig. 24. Model verification curves.

VI. Conclusion

This paper proposes a novel power converter design to drive an SRM machine with a new winding configuration. The objective is to excite portion of the phase windings at high speeds to improve the torque production by overcoming the effect of the high back EMF voltage. The number of turns in stator windings are reduced at the high speeds, while maintaining the high torque density at low speeds by driving the complete number of turns in each phase winding. The proposed method improves the machine characteristics at high speed by enhancing the current controllability that leads to a better average torque production and torque ripple minimization. In the proposed system an extra switch per phase is needed to provide the capability of controlling the excitation current according the speed information. The decision for the number of turns in each portion and the threshold between the high speeds and low speeds was made to optimize the torque production. Different combinations for the number of turns can be applied for the torque improvement and torque ripple minimization objectives.

References

[1] H. Likun, Y. Qingxin, and A. Jinlong, "Modeling of SRM Based on XS-LSSVR Optimized by GDS," *IEEE Trans. Appl. Supercond.,* vol. 20, no. 3, pp. 1102-1105, June 2010.

[2] Y. Hu, X. Song, W. Cao, and B. Ji, "New SR Drive With Integrated Charging Capacity for Plug-In Hybrid Electric Vehicles (PHEVs)," *IEEE Trans. Ind. Electron.,* vol. 61, no. 10, pp. 5722-5731, Oct. 2014.

[3] Y. Hu, C. Gan, W. Cao, W. Li, and S. J. Finney, "Central-Tapped Node Linked Modular Fault-Tolerance Topology for SRM Applications," *IEEE Trans. Power Electron.,* vol. 31, no. 2, pp. 1541-1554, Feb. 2016.

[4] S. Song, M. Zhang, and L. Ge, "A New Fast Method for Obtaining Flux-Linkage Characteristics of SRM," *IEEE Trans. Ind. Electron.,* vol. 62, no. 7, pp. 4105-4117, July 2015.

[5] T. J. E. Miller, "Switched Reluctance Motors and their Control," *Oxford: Magna Physics Publishing And Clarendon Press,* 1993.

[6] D.-H. Lee, and J.-W. Ahn, "A Novel Four-Level Converter and Instantaneous Switching Angle Detector for High Speed SRM Drive," *IEEE Trans. Power Electron.,* vol. 22, no. 5, pp. 2034-2041, Sep. 2007.

[7] I. Husain, "Minimization of Torque Ripple in SRM Drives," *IEEE Trans. Ind. Electron.,* vol. 49, no. 1, pp. 28-39, Feb. 2002

[8] J. L. D.-H Lee, and J.-W. Ahn, "Direct instantaneous torque control of switched reluctance machines using 4-level converters," *IET Electr. Power Appl.,* vol. 3, no. 4, pp. 313-323, Jan. 2008.

[9] C.-H. Yu, and T.-C. Chen, "Novel sensorless driving method of SRM with external rotor using impressed voltage pulse," *IEE Proc.-Electr. Power Appl.,* vol. 153, no. 5, pp. 632-641, 2006.

[10] B. Bilgin, A. Emadi, and M. Krishnamurthy "Comprehensive Evaluation of the Dynamic Performance of a 6/10 SRM for Traction Application in PHEVs," *IEEE Trans. Ind. Elect.,* vol. 60, no. 7, pp. 2564-2575, July, 2013.